Relationship between Vegetation Index and Forest Surface Fuel Load in UAV Multispectral Remote Sensing

Yufei ZHOU*, Zhenshi WANG, Yingxia ZHONG, Qiang LI, Shujing WEI, Sisheng LUO, Zepeng WU, Ruikun DAI, Xiaochuan LI

Guangdong Academy of Forestry, Guangdong Provincial Key Laboratory of Silviculture, Protection and Utilization, Guangzhou 510520, China

Abstract [**Objectives**] To explore the relationship between vegetation index and forest surface fuel load. [**Methods**] UAV multispectral remote sensing was used to obtain large-scale forest images and obtain structural data of forest surface fuel load. This experimental area was located in Gaoming District, Foshan City, Guangdong Province. The average surface fuel load of the experimental area was as high as 39.33 t/ha, and the forest surface fuel load of *Pinus elliottii* was the highest. [**Results**] The normalized difference vegetation index (NDVI) and enhanced vegetation index (EVI) had a moderately strong correlation with the forest surface fuel load. The regression model of NDVI (X) and forest surface fuel load (Y) was established: $Y = -5.935\,4X + 8.466\,3$, and the regression model of EVI (X) and forest surface fuel load (Y) was established: $Y = -5.848\,5X + 6.727\,1$. The study also found that the linear relationship between NDVI and surface fuel load was more significant. [**Conclusions**] Both NDVI and EVI have moderately strong correlations with forest surface fuel load. NDVI is moderately or strongly correlated with the surface fuel load of *Pinus massoniana* forest, shrub grassland, broad-leaf forest and bamboo forest, while EVI is only strongly correlated with surface fuel load of broad-leaf forest and bamboo forest. It is expected that the relationship between other vegetation indices and forest surface fuel load can be obtained by the method in this study, so as to find a more universal vegetation index for calculating surface fuel load.

Key words Unmanned aerial vehicle (UAV), Multispectral remote sensing, Vegetation index, Fuel load

1 Introduction

Forest fuel is the material basis for forest fires[1-2]. When analyzing whether forests can be ignited and studying how forest fires spread and other forest fire behaviors, the fuel is a crucial factor[3-4]. The size of the fuel load directly affects the forest fire behavior such as the burning intensity, flame height, and spreading speed[4-5]. However, the survey of forest fuel load is highly specialized and is subject to the geographical environment, and the field collection workload is large. What's more, work is difficult to implement when a forest fire occurs.

With the aid of satellite images, aerial photos and other multispectral remote sensing data, we can obtain large-scale forest images, to provide the possibility to reduce field survey[6]. With the continuous improvement in the theory of remote sensing technology, the remote sensing data has become more accurate and clear, and using UAV to carry multispectral scanners to survey forest fuel has become a new method and trend[7-8]. At present, researches using UAV multispectral remote sensing mainly focus on the classification of fuels[9-10], but there are relatively few studies on fuel load. UAV airborne Laser Radar (LiDar) can obtain the structure data of surface fuels[11-12], but its modeling operation is relatively complex, and it is difficult for 3D point clouds to have data in every grid like multispectral remote sensing. In this study, we explored the potential relationship between vegetation index and forest surface fuel load in UAV multispectral remote sensing to establish a model between vegetation index and forest surface fuel load.

2 Materials and methods

2.1 Overview of experimental area The experimental area is located in Kengbian Village, Hecheng Town, Gaoming District, Foshan City, Guangdong Province, between 22°57′23″ - 22°57′45″ N and 112°46′45″ - 112°47′10″ E, with an area of 40 ha. It is less than 500 m away from the burned area of the major forest fire in Lingyun Mountain, Gaoming District, Foshan City on December 5, 2019. The experimental area belongs to subtropical monsoon climate zone. The main vegetation includes *Pinus massoniana*, *Pinus elliottii*, *Eucalyptus* spp., *Cinnamomum camphora*, *Schima superba*, *Erythrophleum fordii*, *Castanopsis fissa*, *Castanopsis hystrix*, *Ficus microcarpa*, *Litsea glutinosa*, various shrubs and bamboos, basically covering the main vegetation types in the Gaoming "12.5" major forest fire in Foshan City.

2.2 Arrangement of sample plots and collection of surface fuel load The fuel load is based on the dried fuel load. To verify the relationship between the vegetation index and the actual surface fuel load, we combined the grid sampling method and random sampling method, and set up 50 sample plots with size of 1 m × 1 m each in the experimental area. Among them, 36 plots were set according to 100 m grid, and 14 random plots were set according to different stand types. We collected and bagged all the fuels in the 50 sample plots according to the live fuel and dead fuel. After

Received: June 24, 2022 Accepted: September 19, 2022
Supported by Forestry Science and Technology Innovation Project of Guangdong Province (2018KJCX003).
* Corresponding author. Yufei ZHOU, senior engineer, research direction: forest fire prevention and forestry informationization.

drying, we measured the dried fuel load to establish the surface fuel load model of each stand. The distribution of experimental area and sample plots are shown in Fig. 1.

Fig. 1 Distribution of experimental area and sample plots

2.3 UAV multispectral data collection and vegetation index acquisition We used the Matrice M300 UAV equipped with multispectral and high-definition lenses to collect image data in the experimental area by orthographic projection. The collected multispectral data were stitched using SpectrononPro software after radiometric calibration, reflection correction and geometric correction. Finally, with the aid of ENVI software, we obtained the normalized difference vegetation index (NDVI) (Fig. 2) and enhanced vegetation index (EVI) (Fig. 3) of the experimental area.

3 Results and analysis

3.1 Results According to the vegetation type, we divided the 50 sample plots into *P. elliottii* forest, *P. massoniana* forest, shrub grassland, broad-leaf forest, and bamboo forest types. The location, type, vegetation index, and load of each sample plot are listed in Table 1. The accuracy of orthophoto and plot measured coordinates after RTK correction is within 10 cm, which is enough to meet the requirements of precise correction.

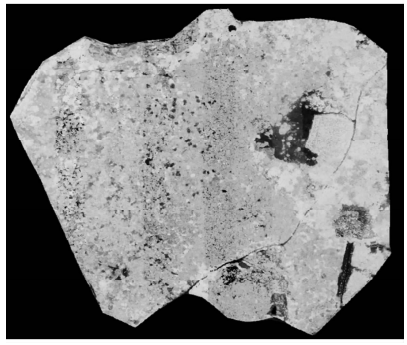

Fig. 2 NDVI of the experimental area

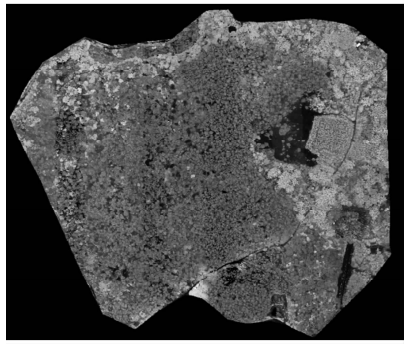

Fig. 3 EVI of the experimental area

Taking the vegetation index as the X-axis, and the surface fuel load as the Y-axis, we plotted the discrete graphs of NDVI and surface fuel load, EVI and surface fuel load, as shown in Fig. 4.

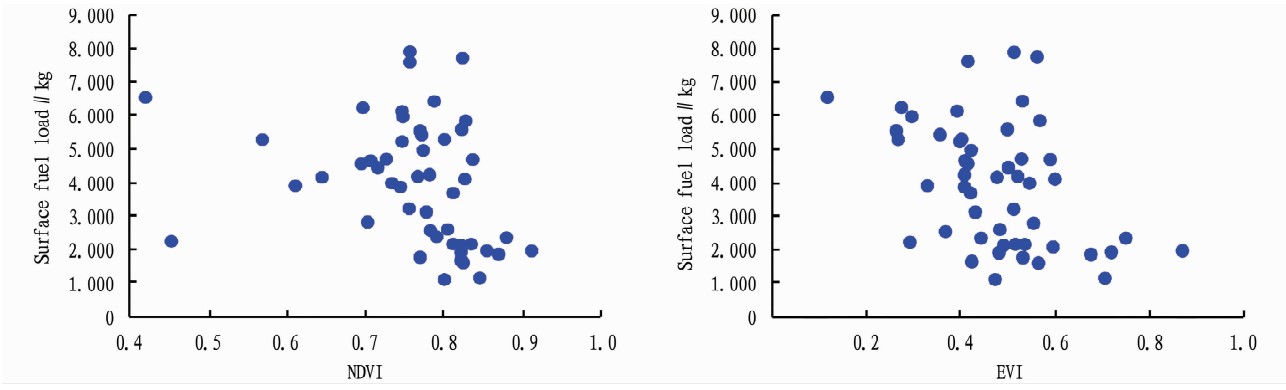

Fig. 4 Discrete graphs of vegetation index and surface fuel load

3.2 Analysis of surface fuel load Using Excel software, we conducted a statistical analysis on the surface fuel load, and the statistical analysis results are shown in Table 2. The dried fuel load of the 50 sample plots was in the range of 1.085 – 7.893 kg, and the average load was 3.933 kg. From the perspective of surface fuel load of various vegetation types, the surface fuel load of *P. elliottii* forest was the highest, followed by *P. massoniana* forest and shrub grassland, and the surface fuel load of broad-leaf forest and bamboo forest was the lowest.

Table 1 Basic information of each sample plot

Type	East longitude	North latitude	NDVI	EVI	Dry weight of live fuel//kg	Dry weight of dead fuel//kg	Load//kg
P. elliottii forest	112°47′0.98″	22°57′25.07″	0.748	0.297	1.225	4.711	5.936
P. elliottii forest	112°46′57.46″	22°57′34.82″	0.716	0.502	0.879	3.546	4.425
P. elliottii forest	112°47′0.98″	22°57′34.82″	0.788	0.532	1.071	5.339	6.410
P. elliottii forest	112°46′50.44″	22°57′38.06″	0.770	0.264	1.036	4.482	5.518
P. elliottii forest	112°47′0.98″	22°57′38.06″	0.734	0.547	0.991	2.976	3.967
P. elliottii forest	112°46′57.46″	22°57′41.31″	0.783	0.366	1.069	1.483	2.552
P. elliottii forest	112°47′0.98″	22°57′41.31″	0.767	0.522	1.291	2.875	4.166
P. elliottii forest	112°47′4.50″	22°57′41.31″	0.782	0.409	1.098	3.115	4.213
P. elliottii forest	112°46′59.26″	22°57′29.85″	0.697	0.275	1.111	5.100	6.211
P. elliottii forest	112°46′57.42″	22°57′36.34″	0.645	0.478	0.714	3.430	4.144
P. elliottii forest	112°46′59.52″	22°57′37.08″	0.757	0.416	0.795	6.778	7.573
P. massoniana forest	112°46′53.95″	22°57′28.32″	0.757	0.515	0.686	7.207	7.893
P. massoniana forest	112°46′57.46″	22°57′28.32″	0.747	0.399	1.050	4.159	5.209
P. massoniana forest	112°47′0.98″	22°57′28.32″	0.825	0.566	0.665	0.923	1.588
P. massoniana forest	112°47′4.50″	22°57′28.32″	0.822	0.492	0.902	1.206	2.108
P. massoniana forest	112°47′4.50″	22°57′28.32″	0.837	0.591	1.054	3.605	4.659
P. massoniana forest	112°46′53.95″	22°57′31.56″	0.569	0.268	1.103	4.163	5.266
P. massoniana forest	112°46′46.92″	22°57′34.82″	0.835	0.537	0.499	1.635	2.134
P. massoniana forest	112°46′50.44″	22°57′34.82″	0.745	0.409	0.757	3.094	3.851
P. massoniana forest	112°46′53.95″	22°57′34.82″	0.824	0.560	1.868	5.832	7.700
P. massoniana forest	112°46′53.95″	22°57′38.06″	0.828	0.569	0.850	4.961	5.811
P. massoniana forest	112°46′57.46″	22°57′38.06″	0.747	0.393	1.040	5.066	6.106
P. massoniana forest	112°46′50.44″	22°57′41.31″	0.791	0.447	0.534	1.822	2.356
P. massoniana forest	112°46′57.46″	22°57′44.56″	0.822	0.482	0.997	0.891	1.888
P. massoniana forest	112°46′51.23″	22°57′29.47″	0.772	0.357	1.155	4.253	5.408
P. massoniana forest	112°46′47.48″	22°57′33.55″	0.812	0.422	1.283	2.384	3.667
Shrub grassland	112°46′53.95″	22°57′25.07″	0.827	0.601	1.566	2.526	4.092
Shrub grassland	112°46′50.44″	22°57′28.32″	0.611	0.330	1.715	2.174	3.889
Shrub grassland	112°47′0.98″	22°57′31.56″	0.774	0.423	0.815	4.123	4.938
Shrub grassland	112°47′4.50″	22°57′38.06″	0.453	0.293	0.876	1.345	2.221
Shrub grassland	112°46′53.95″	22°57′41.31″	0.707	0.41	1.517	3.111	4.628
Shrub grassland	122°46′52.20″	22°57′25.32″	0.801	0.403	1.161	4.115	5.276
Shrub grassland	112°46′52.09″	22°57′26.56″	0.727	0.53	0.820	3.855	4.675
Shrub grassland	112°46′51.95″	22°57′28.54″	0.756	0.512	2.078	1.118	3.196
Shrub grassland	112°46′49.15″	22°57′30.74″	0.695	0.416	1.565	2.969	4.534
Broad-leaf forest	112°47′4.50″	22°57′25.07″	0.812	0.517	1.576	0.561	2.137
Broad-leaf forest	112°47′8.00″	22°57′28.32″	0.823	0.5	0.494	5.070	5.564
Broad-leaf forest	112°46′57.46″	22°57′31.56″	0.822	0.425	0.821	0.839	1.660
Broad-leaf forest	112°47′8.00″	22°57′31.56″	0.801	0.475	0.560	0.525	1.085
Broad-leaf forest	112°47′8.00″	22°57′34.82″	0.770	0.533	1.416	0.330	1.746
Broad-leaf forest	112°46′46.92″	22°57′38.06″	0.912	0.872	0.898	1.035	1.933
Broad-leaf forest	112°46′54.35″	22°57′30.08″	0.420	0.113	1.499	5.027	6.526
Broad-leaf forest	112°47′05.94″	22°57′36.06″	0.846	0.708	0.616	0.517	1.133
Broad-leaf forest	112°47′6.03″	22°57′42.34″	0.855	0.718	1.335	0.601	1.936
Bamboo forest	112°47′4.50″	22°57′31.56″	0.703	0.555	1.469	1.333	2.802
Bamboo forest	112°47′4.50″	22°57′34.82″	0.805	0.484	0.954	1.631	2.585
Bamboo forest	112°47′8.00″	22°57′38.06″	0.822	0.597	0.867	1.190	2.057
Bamboo forest	112°47′8.00″	22°57′41.31″	0.880	0.750	0.953	1.382	2.335
Bamboo forest	112°47′3.36″	22°57′31.49″	0.870	0.677	0.544	1.291	1.835
Bamboo forest	112°47′5.13″	22°57′41.26″	0.778	0.432	1.764	1.334	3.098

Table 2 Statistical analysis of surface fuel load

Type	Number of plots	Sum	Max	Min	Mean	Variance
P. elliottii forest	11	55.115	7.573	2.552	5.010	1.437
P. massoniana forest	15	65.644	7.893	1.588	4.376	2.072
Shrub grassland	9	37.449	5.276	2.221	4.161	0.951
Broad-leaf forest	9	23.720	6.526	1.085	2.636	1.980
Bamboo forest	6	14.712	3.098	1.835	2.452	0.471
All type	50	196.640	7.893	1.085	3.933	1.835

For the surface fuel load of each vegetation type and other vegetation types, we carried out the difference significance test, and mainly the T test to calculate the P. The test results are shown in Table 3. In general, the P of the T test can indicate whether there is a significant difference. In statistics, when the P is less than 0.05, the difference is significant; when the P is less than 0.01, the difference is extremely significant; when the P is greater than 0.05, the difference is not significant[13]. From Table 3, it can be seen that the difference in surface fuel load between bamboo forest and other vegetation types was extremely significant; the difference between *P. elliottii* forest and broad-leaf forest and other vegetation types was significant, the difference between *P. massoniana* forest and shrub grassland and other vegetation types was not significant, which is possibly because the species of surface vegetation in *P. massoniana* forest and shrub-grassland are more abundant, and the difference in species of surface vegetation is different, leading to large fluctuation of the fuel load.

Table 3 Significance test of load difference (P value)

Type	*P. elliottii* forest	*P. massoniana* forest	Shrub grassland	Broad-leaf forest	Bamboo forest
Dry weight of live fuel	0.485	0.164	0.061	0.713	0.909
Dry weight of dead fuel	0.013	0.183	0.909	0.054	$2.56E^{-7}$
Load	0.016	0.309	0.536	0.049	$2.29E^{-5}$

3.3 Analysis of the relationship between vegetation index and surface fuel load The Pearson correlation coefficient (Pearson's r, hereafter referred to r) is usually used in statistics to measure the degree of linear correlation between two sets of data[14]. In this study, we used r to measure the degree of linear correlation between vegetation index and various types of surface fuel load, and its r value is shown in Table 4.

Table 4 Vegetation index and r value of various vegetation types of surface fuel load

Type	*P. elliottii* forest	*P. massoniana* forest	Shrub grassland	Broad-leaf forest	Bamboo forest	All type
NDVI	0.036	−0.305	0.720	−0.710	−0.710	−0.303
EVI	−0.260	−0.089	0.274	−0.632	−0.729	−0.434

Generally, if the absolute value of r is in the range of 0 − 0.09, it indicates that the two sets of data are not correlated; if the absolute value of r is in the range of 0.1 − 0.3, it indicates that the two sets of data are weakly correlated; if the absolute value of r is in the range of 0.3 − 0.5, it indicates that the two sets of data are moderately correlated; if the absolute value of r is in the range of 0.5 − 1.0, it indicates that the two sets of data are strongly correlated[15]. From Table 5, it can be seen that NDVI and EVI had a moderate correlation with the surface fuel load; NDVI had a strong correlation with the surface fuel load of shrub grassland, broad-leaf forest and bamboo forest; EVI had a strong correlation with the surface fuel load of broad-leaf forest and bamboo forest; NDVI had a moderate correlation with the surface fuel load of *P. massoniana* forest; the correlation between other vegetation types and vegetation index was small.

For the two sets of data with moderate intensity and strong correlation, using X to represent the vegetation index value and Y to represent the surface fuel load, we can fit a linear function (Equation 1). We established the linear regression model of NDVI and surface fuel load (Equation 2):

$$Y = -5.935\,4X + 8.466\,3 \quad (1)$$

The linear regression model of EVI and surface fuel load:

$$Y = -5.848\,5X + 6.727\,1 \quad (2)$$

The fitting functions of surface fuel load of other vegetation types and vegetation index are shown in Table 5.

Table 5 Fitting functions of surface fuel load and vegetation index for each vegetation type

Vegetation index	Type	Fitting function of surface fuel load (X) and vegetation index (Y)	Correlation
NDVI	*P. massoniana* forest	$Y = -9.219\,4X + 11.588$	Moderate
NDVI	Shrub grassland	$Y = 5.996\,8X - 0.070\,7$	Strong
NDVI	Broad-leaf forest	$Y = -9.874\,3X + 10.383$	Strong
NDVI	Bamboo forest	$Y = -5.143\,3X + 6.616\,4$	Strong
EVI	Broad-leaf forest	$Y = -5.799\,4X + 5.767\,9$	Strong
EVI	Bamboo forest	$Y = -2.895\,6X + 4.138\,7$	Strong

(To page 41)

tooning agro-system: Which one is more environment-friendly[J]. Environmental Science and Pollution Research, 2018, 25: 32246 – 32256.
[9] ALIZADEH MR, HABIBI F. A comparative study on the quality of the main and ratoon rice crops[J]. Journal of Food Quality, 2016, 39(6): 669 – 674.
[10] XU XB, CHEN L, QIAN TP, *et al.* Comparative experiment of mechanical harvesting and manual harvesting in ratooned rice season[J]. China Seed Industry, 2016, (11): 52 – 53. (in Chinese).
[11] PENG SB. Booming research on rice physiology and management in China: A bibliometric analysis based on three major agronomic journals[J]. Journal of Agricultural Sciences, 2017, 16(12): 2726 – 2735. (in Chinese).
[12] ZHOU W, WANG WH, ZHENG PB, *et al.* Application of wide and narrow row cultivation technology on ratooned rice[J]. China Rice, 2019, 25(2): 72 – 74. (in Chinese).
[13] ZHU JM, CHEN HP, YIN H. Study on green and efficient cultivation model of first season rice-ratooned rice-rapeseed (green manure)[J]. Southern Agriculture Journal, 2020, 14(24): 30 – 31, 42. (in Chinese).
[14] ZOU JN, GAN GY, ZHANG X, *et al.* Research progress on nitrogen literacy management in ratooned rice cultivation[J]. Southern Agriculture Journal, 2020, 14(25): 31 – 34. (in Chinese).
[15] HUANG SH, LIN XY, LEI ZP, *et al.* Physiological characteristics of carbon and nitrogen nutrition and hormones of rice cultivars with strong ratooning power[J]. Acta Agronomica Sinica, 2021, 47(11): 2278 – 2289.

(From page 36)

4 Conclusions and discussion

The average load of 50 sample plots is 3.933 kg or 39.33 t/ha, which exceeds the critical value of 30 t/ha for major forest fires[16], indicating that the surface fuel load in the experimental area is very high. Among them, the surface fuel load of *P. elliottii* forest is the highest, and the surface fuel load of broad-leaved forest and bamboo forest is lower. The difference in surface fuel load between bamboo forest and other vegetation types is extremely significant; the difference in surface fuel load between *P. elliottii* forest and broad-leaf forest and other vegetation types is significant; the surface fuel load of *P. massoniana* forest and shrub grassland is not significantly different from that of other vegetation types due to the large differences in surface vegetation populations.

Both NDVI and EVI have a moderate correlation with the surface fuel load, indicating that the models corresponding to surface fuel load can be constructed to a certain extent. We established the two models of vegetation index and surface fuel load, as shown in equations (1) and (2). The NDVI is moderately or strongly correlated with the surface fuel load of *P. massoniana* forest, shrub grassland, broad-leaf forest and bamboo forest, while the EVI only has a strong correlation with the surface fuel load of broad-leaf forest and bamboo forest, which indicates that the use of NDVI can establish a more linear relationship with the surface fuel load.

In this study, we only collected relevant data in the same area, and only collected data from 50 sample plots, it is necessary to collect data from more sample plots in more different regions to make the conclusions more representative and universal. Since there are many types of vegetation indices, the relationship between other vegetation indices and surface fuel load can be further obtained by the method in this study, so as to find a more universal vegetation index for calculating the surface fuel load.

References

[1] HU HQ, LUO SS, LUO BZ, *et al.* Forest fuel moisture content and its prediction model[J]. World Forestry Research, 2017, 30(3): 64 – 69. (in Chinese).
[2] LI BY, SHU LF, DING YQ, *et al.* Research progress in plantation fuel characteristics and management in China[J]. World Forestry Research, 2021, 34(1): 90 – 95. (in Chinese).
[3] ZONG XZ, TIAN XR. Research progress in forest fire behavior and suppression technology[J]. World Forestry Research, 2019, 32(6): 31 – 36. (in Chinese).
[4] HE HS, CHANG Y, HU YM, *et al.* Contemporary studies and future perspectives of forest fuel and fuel management[J]. Chinese Journal of Plant Ecology, 2010, 34(6): 741 – 752. (in Chinese).
[5] WANG QH, SHU LF, DAI XA, *et al.* Effects of snow and ice disasters on forest fuel and fire behaviors in the southern China[J]. Scientia Silvae Sinicae, 2008, 44(11): 171 – 176. (in Chinese).
[6] WANG ZS, ZHOU YF, LI XC, *et al.* Application analysis of UAV in forest fire prevention[J]. Guangdong Forestry Science and Technology, 2016, 32(1): 31 – 35. (in Chinese).
[7] WU C, XU WH, HUANG SD, *et al.* Research progress of remote sensing for forest-fire monitoring[J]. Journal of Southwest Forestry University, 2020, 40(3): 172 – 179. (in Chinese).
[8] REILLY S, CLARK ML, BENTLEY LP, *et al.* The potential of multispectral imagery and 3D point clouds from unoccupied aerial systems (UAS) for monitoring forest structure and the impacts of wildfire in Mediterranean-climate forests[J]. Remote Sensing, 2021, 13(19): 3810.
[9] LI XT, QIN XL, LIU Q, *et al.* An identification method on forest fuel types based on AISA Eagle II hyperspectral data[J]. Remote Sensing Technology and Application, 2021, 36(3): 544 – 551, 570. (in Chinese).
[10] FUJIMOTO A, HAGA C, MATSUI T, *et al.* An end to end process development for UAV-SfM based forest monitoring: Individual tree detection, species classification and carbon dynamics simulation[J]. Forests, 2019, 10(8): 680.
[11] HILLMAN S, WALLACE L, LUCIEER A, *et al.* A comparison of terrestrial and UAS sensors for measuring fuel hazard in a dry sclerophyll forest[J]. International Journal of Applied Earth Observation and Geoinformation, 2021, 95: 102261.
[12] ZHOU YF, WANG ZS, ZHONG YX, *et al.* Estimation technology of eucalyptus stock volume on UAV-based LiDAR[J]. Guangdong Forestry Science and Technology, 2021, 37(2): 7 – 11. (in Chinese).
[13] WANG ZW, XIE HG. Probability Theory and Mathematical Statistics[M]. Beijing: China Forestry Publishing House, 2010. (in Chinese).
[14] HUANG QX. Response and trend forecast of forest fires in Fujian Province to climate change[D]. Fuzhou: Fujian Agriculture and Forestry University, 2020. (in Chinese).
[15] CHEN XR. Probability Theory and Mathematical Statistics[M]. Hefei: University of Science and Technology of China Press, 2017. (in Chinese).
[16] National Forestry and Grassland Administration. National Action Plan on Forest Fires (2016 – 2025). [EB/OL]. http://www.gov.cn/xinwen/2016-12/29/content_5154054.htm, 2016-12-19/2022-03-20. (in Chinese).